Evaluation of X-ray target materials to improve CT-based measurement of fiber orientations inside CF-SMC components

Jan TEUWSEN [1], Florian BITTNER [2], Jens Peter STEFFEN [3]
[1] Volkswagen AG, D-38436 Wolfsburg, Germany
[2] Fraunhofer Institute for Wood Research WKI, D-30453 Hannover, Germany
[3] X-RAY WorX GmbH, D-30827 Garbsen, Germany

Contact e-mail: jan.teuwsen@volkswagen.de

Abstract. Carbon fiber sheet molding compounds (CF-SMC) are increasingly used in automotive and aerospace industries. The accuracy of fiber orientation measurement depends on the quality of the computed tomography (CT) results. This is significantly influenced by signal and contrast obtained when imaging the low absorption materials. Using standard tungsten X-ray targets as available in most commercially available microfocus CT scanners appears to be a compromise in terms of contrast and flux.

The authors compare the X-ray spectra and imaging properties achieved using tungsten, copper, and silver X-ray targets. Projections and volume data sets obtained from scanning a CF-SMC sample component using different X-ray targets are compared and evaluated using common quantities like grey value distribution and signal-to-noise ratio. Finally, the different volumes are analyzed by using a common software module and fiber orientation tensors are compared.

1. Introduction

Over the last decades, compression molded discontinuous fiber composites (DFC) such as carbon fiber sheet molding compounds (CF-SMC) have been used extensively for interior and exterior, structural and non-structural composite applications in automotive and aerospace industry [1] [2]. High performance CF-SMCs, such as the materials used in this study (see section *2.1 Materials*), are characterized by a high delamination resistance, near quasi-isotropic in-plane stiffness, high out-of-plane strength and stiffness, and low notch sensitivity [3]. The epoxy-based CF-SMC HexMC has a very short curing time, leading to a 84 % shorter molding time and an overall process time reduction of 44 % for a large part (monocoque tub) compared to the same part produced in a resin transfer molding (RTM) process [4]. In comparison to the RTM process, the easy and time saving compression molding process leads to lower costs and also reduces the final amount of parts due to the chance of part integration (fasteners, inserts) [1]. Since CF-SMC is suitable for high volume production at low manufacturing costs and enables molding of complex three-dimensional (3D) geometries [1], lightweight components made of CF-SMC are used for many industry applications like window frames [2] [3], body panels, interior trims, seats, engine bay covers and braces [5], handles, air intakes, central tunnel claddings, inner monocoques, suspension control arms, and several other cockpit parts for example in the latest Lamborghini research and serial cars (Sesto Elemento, Veneno, Aventador, Huracán, and Urus) [3] [6] [7] [8].

Due to the part design and the manufacturing process a characteristic microstructure is induced in CF-SMC components. This process-induced microstructure is mainly characterized by a locally varying fiber orientation and fiber concentration determining the part's mechanical properties. The DFC materials used in this study consist of thermoset resins reinforced by transversely chopped carbon fiber tows ('strands', also called 'chips' or 'platelets' in literature) which are randomly distributed into a mat. The long carbon fibers are strongly aligned in longitudinal direction of the strands. Materials with those randomly oriented strands (ROS) are characterized by a high degree of heterogeneity (variability in intra- and inter-part structure on the meso- and macro-scale) and seek to reach quasi-isotropic mechanical properties [3] [9] [10]. Therefore, obtaining a realistic three-dimensional representation of the local fiber orientations in a CF-SMC part is key for a better understanding of the compression molding process, to be able to validate compression molding process simulations or to map the gained fiber orientation information into a structural mesh of an integrative (coupled) Finite Element Analysis (FEA) [11] [12]. In order to ensure a proper component design regarding mechanical requirements and for quality assurance of manufactured composite parts, the industry's endeavor is to determine the material's microstructure for large areas or ideally for an entire part [12].

In order to collect experimental 3D information about fiber orientation distributions of heterogeneous fiber reinforced materials (such as CF-SMC), X-ray computed tomography (CT) is widely used in industry due to the fact that it is easy to prepare samples and only requires a difference in the linear X-ray attenuation coefficients of the matrix and the reinforcement [13]. The inner structure/morphology of inhomogeneous materials like CF-SMCs can be investigated three-dimensionally by micro-CT (μ-CT), which is a high resolution X-ray computed tomography method, allowing an in-depth material characterization [13].

However, due to the lack of X-ray contrast between epoxy or vinyl ester resins and carbon fibers, μ-CT scans are so far not useable to scan larger CF-SMC components and still receive useful fiber orientation data. Obtaining CT data for an entire 3D part is always a trade-off between scan volume size, possible resolution (voxel size) and the required scanning time. Normally, attaining fiber orientations by CT scan data analysis of fiber reinforced polymer parts requires a finer scan resolution than the fiber's diameter, which by implication limits the scan volume size [14].

Useful μ-CT scans for CF-SMC parts need a sufficient resolution so that it is clearly distinguishable between strands and resin by grey value differences enabling a fiber orientation analysis with a common CT scan analysis software (e. g. VGStudio MAX, Volume Graphics GmbH, Heidelberg, Germany). The analysis algorithm within VGStudio MAX is intended to be used for the orientation analysis of discretely visible fibers [11] [15] [16] [17] [18]. Yet with correctly set parameters and with local relative density gradients between resin and fibers the image analysis principles are suited to be used for scans with meso-scale resolutions where no single fibers, only coarser structures like fiber strands and fiber bundles, respectively, are visible [12] [13]. Since microscopy shows that during compression molding the fibers within one strand flow and orient together, deforming yet remaining as an intact strand with locally highly aligned fibers, the density gradients of CT scanned ROS-based materials are sufficient for a determination of local average strand orientations even at a coarser scan resolution [11] [12] [13] [19]. In a CT scan of a ROS-based material the smallest density gradient is present in in-strand-direction (along the fibers), intermediate density differences are visible transverse to the strand orientation and the highest density gradient occurs normal to the strand direction [13].

Denos uses a CT scan with a meso-scale resolution of 53 µm (voxel edge length) to determine the heterogeneous internal microstructure of a 65 x 65 x 45 mm^3 strand-based long discontinuous fiber composite part [11] [20]. However, at that resolution and with the used CT scan settings it is not possible to distinguish between single carbon fibers (⌀ ≈ 7 µm) and the matrix or to discern strand boundaries (~ 100 µm thick) [11]. Although Denos' CT scan configuration is not able to represent distinct strand boundaries, it is still possible to receive a mean local fiber orientation [11].

Another common method to achieve bigger CT scan volumes at a reasonable resolution is to merge several scan volumes generating a digital twin of the scanned part and it's microstructure. Kravchenko merged 8 scans with a volume of 30 x 30 x 5 mm^3 each, using a scan resolution of 15 µm [13]. At that resolution the CT scan quality is high enough to discern between strands and suitable for reasonable fiber orientation analyses. Kravchenko uses an analysis mesh size of 0.7 x 0.7 x 0.1 mm^3, where each grid element contains about 13,000 voxels, which are used to determine a single orientation tensor from each of the measured orientation vectors by a grey scale analysis [13]. The finer analysis resolution in thickness direction better resolves the thin strands and enables gathering more detailed information about the local strand orientation changes.

The spectrum generated by the X-ray source significantly depends on the elemental composition of the used target material. Tungsten (W) is widely used as target material for microfocus X-ray sources. However, depending on the applied X-ray voltage and the absorption behavior of the sample material, alternative target materials might deliver beneficial spectrum characteristics that can improve CT measurement quality concerning the separation capability of fiber and matrix for fiber orientation analysis. A higher µ-CT scan quality, by means of a higher contrast between fiber and matrix, also enables to scan bigger composite part volumes, fulfilling industry demands, where the fiber orientation within a whole component is of interest.

To study the effect of copper (Cu) and silver (Ag) targets in comparison to a standard tungsten (W) target in µ-CT scans different carbon/epoxy composite samples are measured with different voxel resolutions. Furthermore, X-ray source resolution, grey value distribution as well as subjective image quality of the CT data are examined and comparative fiber orientation analyses are performed.

2. Experiments

2.1 Materials

The high performance CF-SMCs examined in this study are Hexcel's HexMC® and A. Schulman's Quantum AMC® 8593 HT. Both materials are designed for compression molding of complex shaped parts in a heated metal tool. HexMC® is a DFC which consists of unidirectional (UD) preimpregnated (prepreg) AS4/8552 carbon-epoxy tapes that are slit longitudinally and chopped transversely into strands and then randomly distributed into a mat [9] [10] [3]. Those ROS have nominal in-plane dimensions of 50 mm x 8 mm (2 in x 0.3 in) and a thickness of approximately 0.15 mm containing high strength carbon fibers impregnated by a fast curing Hexcel HexPly® M77 epoxy resin. The carbon fiber content is 62 % by weight, corresponding to 57 % fiber volume content and giving a material density of 1.55 g/cm^3.

A. Schulman's Quantum AMC® 8593 HT is a vinyl ester based SMC containing chopped 25 mm long PAN based 3 K carbon fiber tows [21]. The carbon fiber weight content is 50 %, giving a material density of 1.45 g/cm^3.

The samples analyzed in this study were cut out of plates (320 x 320 x 3.8 mm) (**Fig. 1** and **Fig. 2**) that were manufactured with a high mold coverage of 94 % (low- to no-flow conditions) in a 1000 ton (Dieffenbacher DCL 1000) compression molding machine at a temperature of 135 °C, a pressure of 110 bar, a closing speed of 16 mm/s, and a closing time of 480 s.

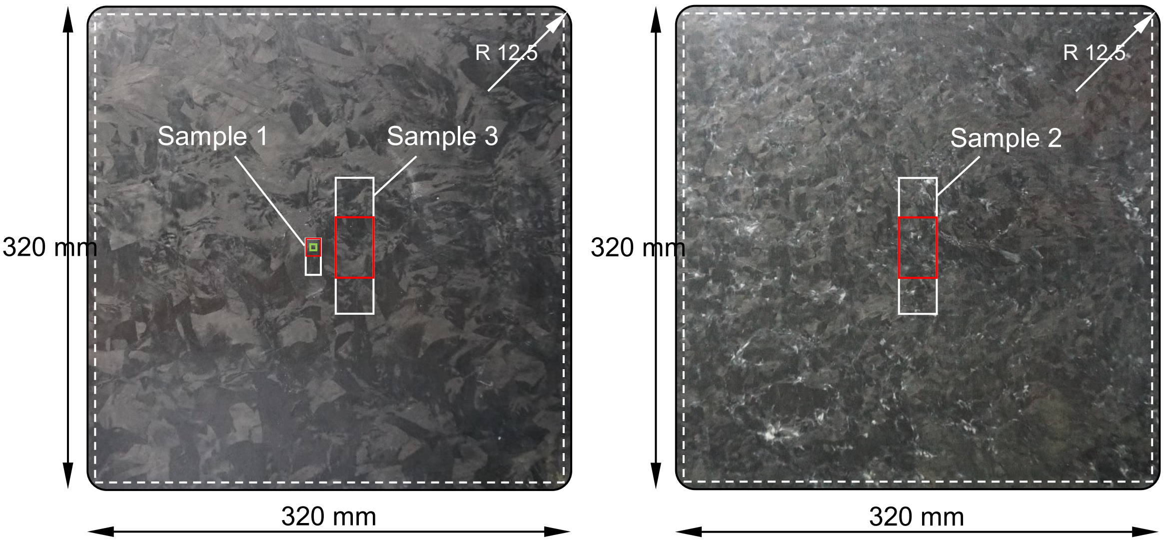

Fig. 1. Used SMC plates (left: HexMC; right: AMC), position of the 310 x 310 mm initial raw material charges (dotted white boxes) and location of cut out material samples (white boxes). Colored boxes denote CT analysis regions.

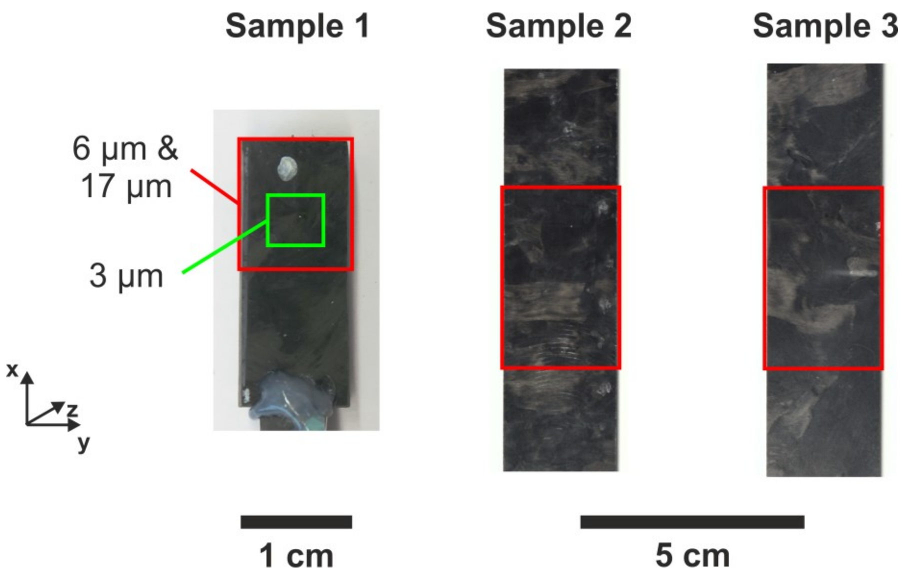

Fig. 2. Cut out material samples (colored boxes denote CT analysis regions with different scan resolutions)

2.2 Micro-CT Measurements

The CT measurements of three CF-SMC samples were performed on a CT-AlphaDuo device (Procon X-Ray GmbH, Sarstedt, Germany) operated by the Fraunhofer WKI, Hannover, Germany. The system is equipped with a 240 kV microfocus X-ray source XWT-240-TCHE Plus (X-RAY WorX GmbH, Garbsen, Germany) and a PaxScan® 2530DX detector (Varian Medical Systems, Inc., Salt Lake City, Utah, USA). While sample 1 was scanned with the three selected target materials and in different resolutions, for sample 2 and 3 only the target material was varied. The applied scan parameters are given in **Tab. 1**. To achieve comparable exposures of the X-ray images for the different targets the exposure time was adjusted. To maximize the scan resolution of the high aspect ratio samples scans at a voxel resolution of 6 and 17 µm were performed in helix mode. The scan of sample 1 at a resolution of 2.9 µm was performed in conventional axial mode. At the same resolution identical sample volumes were captured. For visualization and analysis of the volume data VGSTUDIO MAX 3.2 (Volume Graphics GmbH, Heidelberg, Germany) was used.

Tab. 1. Micro-CT measurement parameters

	Target material	Voxel resolution [µm]	X-ray voltage [kV]	X-ray current [µA]	FDD [mm]	Exposure time [ms]	Measuring time [min]	Approx. I_0 value [-]
Sample 1 (HexMC)	W	2.9	50	75	1000	8 x 3000	960	30,500
	W	6.3	65	140	600	8 x 300	135	35,000
	Cu	6.1	65	140	600	8 x 500	225	31,500
	Ag	6.1	65	140	600	8 x 300	135	36,700
	W	17.4	65	350	700	8 x 200	75	42,200
	Cu	17.4	65	350	700	8 x 300	115	33,250
	Ag	17.3	65	350	700	8 x 200	75	44,800
Sample 2 (AMC)	W	17.4	65	350	700	8 x 200	85	43,600
	Cu	17.4	65	350	700	8 x 400	170	44,000
	Ag	17.3	65	350	700	8 x 200	85	44,000
Sample 3 (HexMC)	W	17.4	65	350	700	8 x 200	90	42,800
	Cu	17.4	65	350	700	8 x 400	180	45,000
	Ag	17.4	65	350	700	8 x 200	90	43,600

2.3 JIMA Resolution Tests

To determine the effective image resolution of the selected setups, the JIMA resolution pattern RT RC-02B [22] was imaged at the same settings that were used for the particular CT scans. This includes target type, X-ray parameters, focus-to-detector distance (FDD), magnification, and exposure time for the single projection. The tested parameters and effective resolutions are listed in **Tab. 2**. The JIMA resolution was selected as the smallest pattern size showing at least 10 % variation of the estimated modulation transfer function (MTF) between the lines and spaces [23].

Tab. 2. JIMA resolution test parameters and determined resolution

Target material	X-ray voltage [kV]	X-ray current [µA]	FDD [mm]	Magni-fication	Exposure time [ms]	Effective resolution [µm]
W	65	140	600	80 x	8 x 300	7
Cu	65	140	600	80 x	8 x 500	7
Ag	65	140	600	80 x	8 x 300	7
W	65	350	700	95 x	8 x 200	15
Cu	65	350	700	95 x	8 x 300	15
Ag	65	350	700	95 x	8 x 200	15

2.4 X-Ray Spectra Simulations of Different Transmission Targets

The software *aRTist 2.10* published by Bundesanstalt für Materialforschung und -prüfung (BAM, Berlin) [24] was used to simulate the X-ray spectra of the three transmission targets applied in this study (**Fig. 3**). The simulation was performed for a voltage of 65 kV. At this energy the resulting tungsten spectrum does not exhibit the characteristic K-shell emission lines. The highest bremsstrahlung radiation in the considered energy range is delivered by the silver target which also gives the most significant contribution of the K-shell emission lines at 22 and 25 keV.

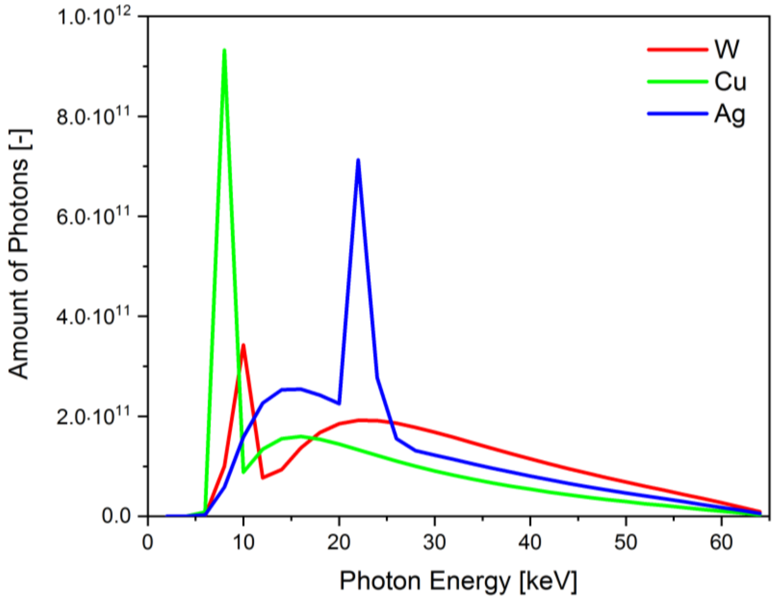

Fig. 3. Simulated spectra of tungsten target, copper target, and silver target

3. Results and Discussion

To investigate whether the different target materials have an effect on the ability to differentiate fiber and matrix, sample 1 was scanned with different voxel resolutions and fiber orientation analyses were applied to the same sample region. The fiber orientation tensors obtained from the scan with the W target at the highest resolution (2.9 µm) serve as reference for the other scan parameters. Samples 2 and 3 with slightly different compositions have larger sample dimensions than sample 1 and serve as demonstrators for application-orientated case studies.

In contrast to the standard W target a grey value analysis of the reconstructed volume data (**Tab. 3**) generally shows a shift of the grey values towards higher values by usage of Cu and Ag as target materials. Although the relative distance between the fiber and the matrix signals does not change significantly, the wider spreading of the grey value spectrum should principally improve the ability to separate fiber and matrix for fiber orientation measurements. For copper the higher grey values in exchange require higher measuring times due to the lower X-ray intensity.

JIMA resolution tests (cf. **Tab. 2**) have verified the resolution of the X-ray source for the different target materials and X-ray parameters. With 7 and 15 µm, respectively, it is comparable to the nominal voxel size of the CT scans. No difference in JIMA resolution is noticeable for the different target materials.

Tab. 3. Grey value distribution in dependence on target material

Sample	Target material	Voxel resolution [µm]	Avg. grey value matrix	Avg. grey value fiber	Relative difference grey value fiber/matrix [%]
Sample 1 (HexMC)	W	2.9	1127	1570	28.2
	W	6.3	1446	1737	16.8
	Cu	6.1	2489	2916	14.6
	Ag	6.1	2229	2644	15.7
	W	17.4	1308	1527	14.3
	Cu	17.4	1350	1520	11.2
	Ag	17.3	3366	3866	12.9
Sample 2 (AMC)	W	17.4	7160	8003	10.5
	Cu	17.4	8460	9564	11.5
	Ag	17.3	7790	8943	12.9
Sample 3 (HexMC)	W	17.4	2987	3376	11.5
	Cu	17.4	3600	4039	10.9
	Ag	17.4	3352	3845	12.8

The general effect of voxel resolution on detectable details is visible in **Fig. 4**, where sectional images at the same positions of sample 1 are compared for voxel sizes of 3, 6 and 17 µm. With a voxel resolution of 3 µm individual carbon fibers can be detected. The fiber orientation is clearly recognizable. This detail detectability at a voxel resolution of 3 µm gives reason to expect a plausible representation of the real fiber orientations of the sample, when a fiber orientation analysis is performed on these data.

When a voxel resolution of 6 µm is applied, individual carbon fibers are still visible, but the discrimination of fibers inside the strands deteriorates. For a resolution of 17 µm no single fibers are recognizable. The structure and orientation of the strands and their layered structure is still visible.

While the grey value gradients, which are detectable in a scan with a voxel size of 6 or 17 µm allow the execution of a fiber orientation analysis for this type of material, the loss of details unquestionably implicates an increased inaccuracy of the results. An evaluation of the accuracy of the obtained orientation vectors, that is required for the conduction of structural mechanics simulation, is out of the scope of this work. Therefore only a qualitative comparison of detail detectability and obtained fiber orientations in dependence on the target material is conducted.

Fig. 5 to **Fig. 8** compare sectional images of the different samples and voxel resolutions for the different target materials. Only slight differences in the image quality are observable. The scans of sample 1 acquired with the Ag target (**Fig. 5** and **Fig. 6**) appear to feature less noise than the scans with the W and Cu target. This is most notably in the areas occupied by matrix, which should be a homogeneous area without structures. While the noise level in all measurements of sample 2 and 3 (**Fig. 7** and **Fig. 8**) appears comparable, the edge contrast between strands and resin appears more distinct for the Cu and Ag target than for the W target. Both a lower noise level and a higher contrast between fiber and matrix would be beneficial for fiber orientation analyses.

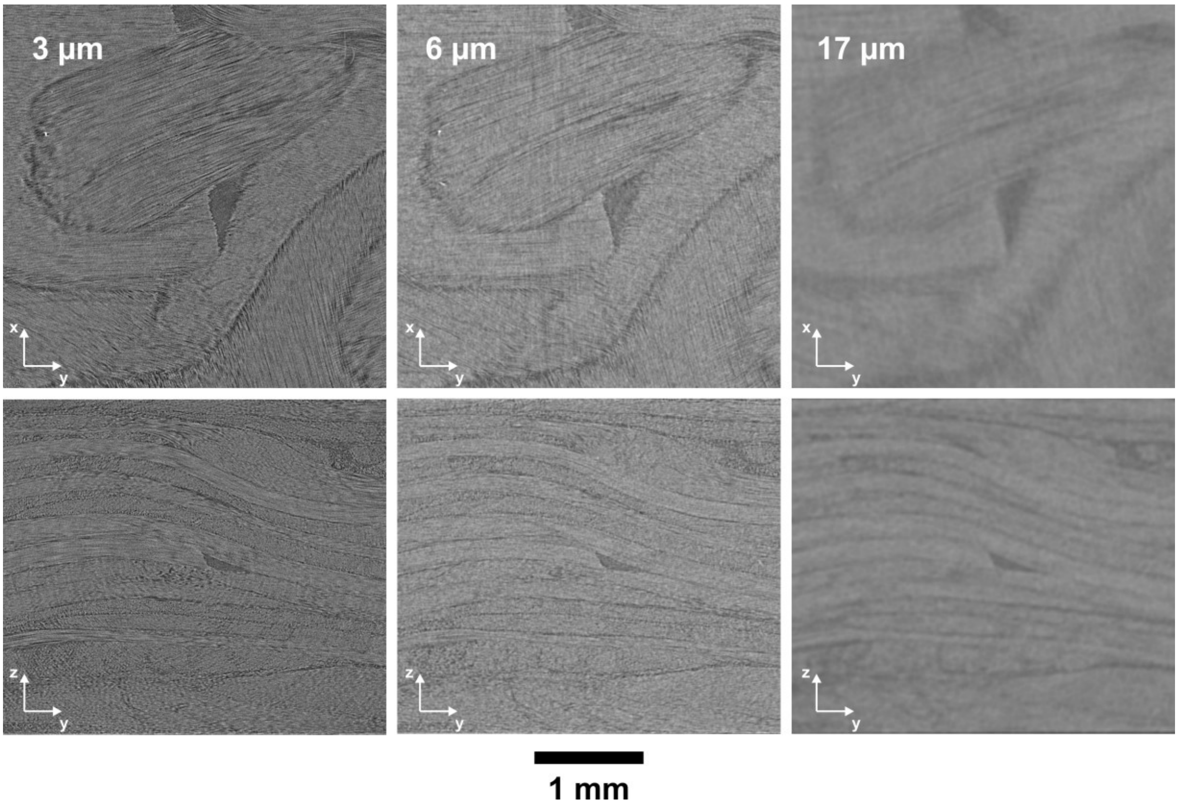

Fig. 4. Cross-sectional CT images of sample 1 at different voxel resolutions, W target; top: in-plane view, bottom: through-thickness view

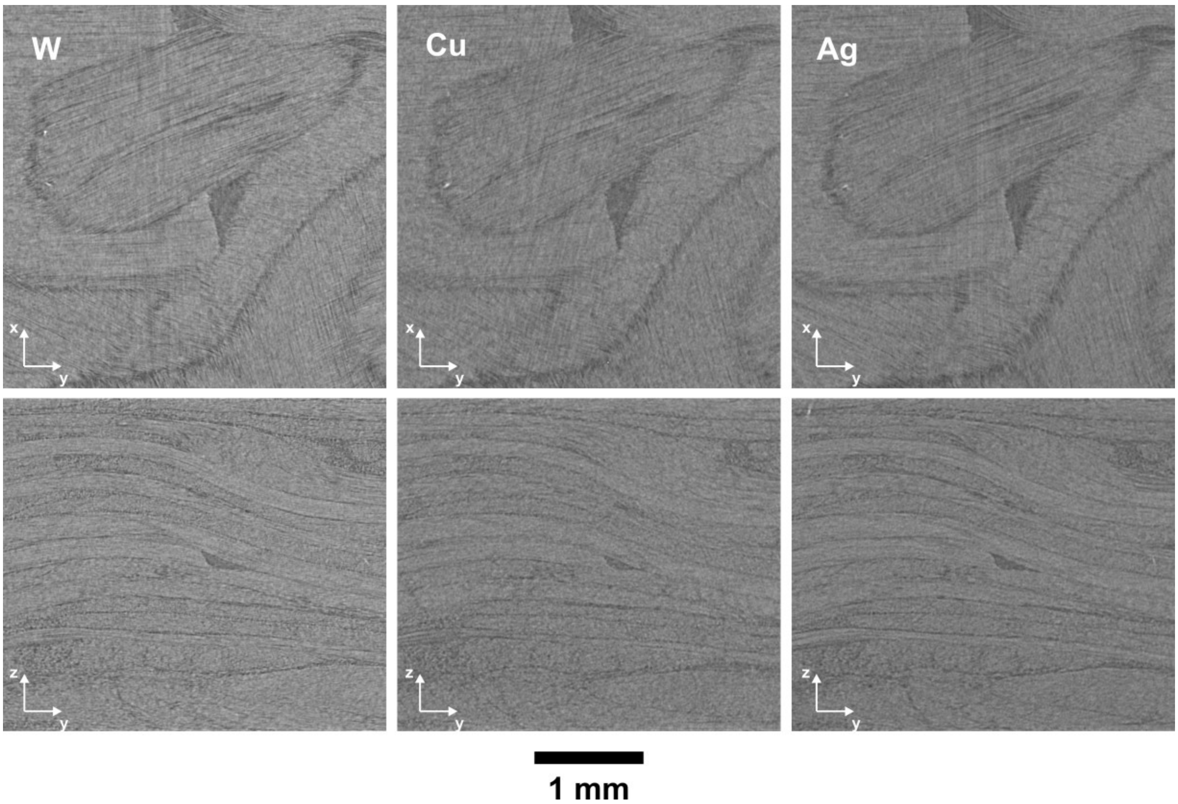

Fig. 5. Comparison of different target materials for sample 1 at a voxel resolution of approx. 6 µm; top: in-plane view, bottom: through-thickness view

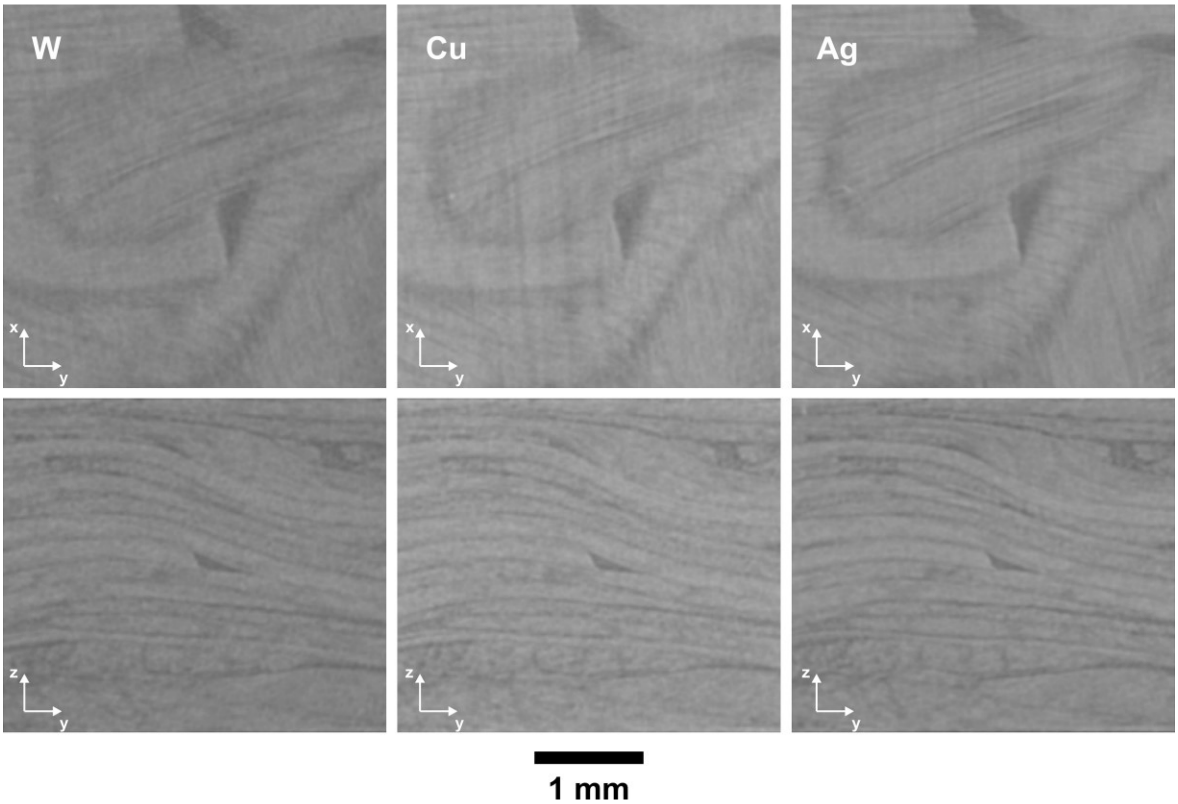

Fig. 6. Comparison of different target materials for sample 1 at a voxel resolution of approx. 17 µm; top: in-plane view, bottom: through-thickness view

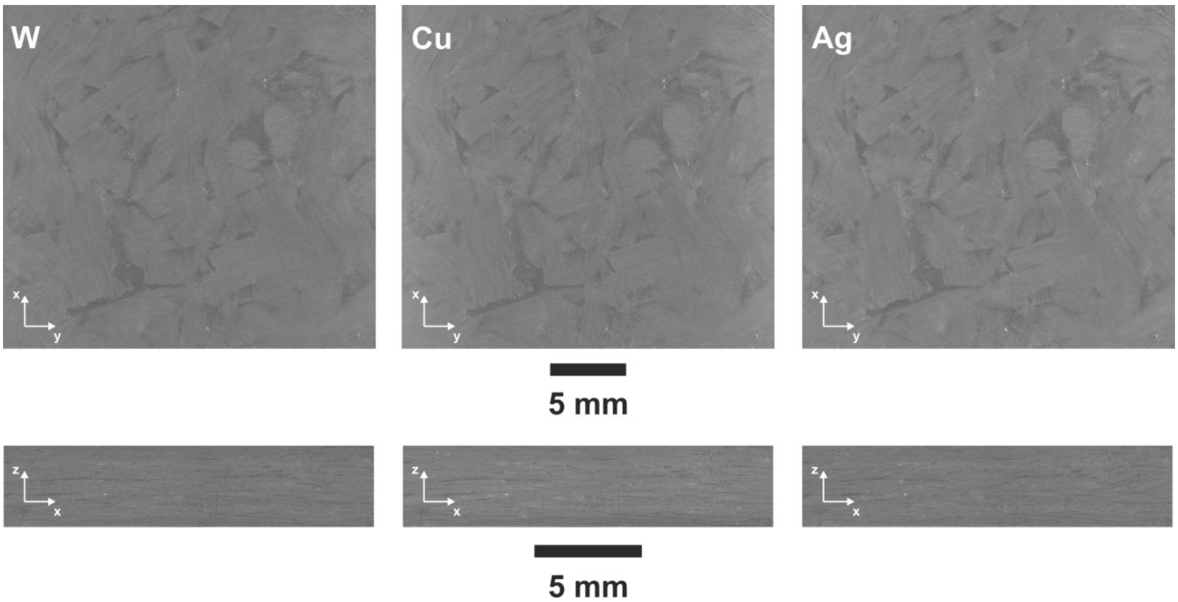

Fig. 7. Comparison of different target materials for sample 2 at a voxel resolution of approx. 17 µm; top: in-plane view, bottom: through-thickness view

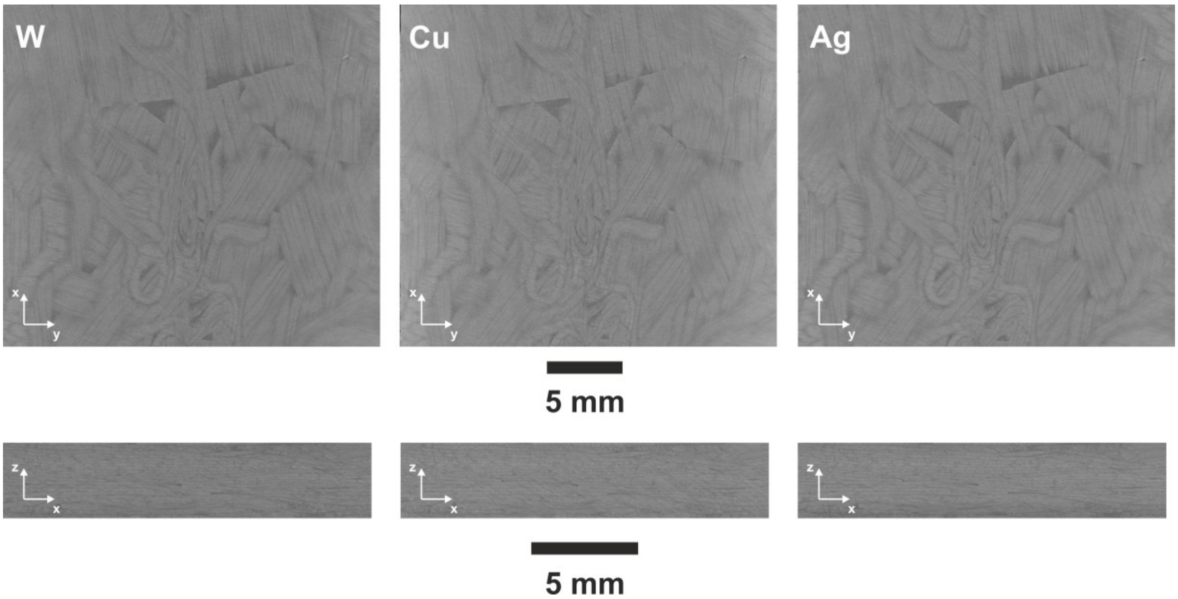

Fig. 8. Comparison of different target materials for sample 3 at a voxel resolution of approx. 17 µm; top: in-plane view, bottom: through-thickness view

Fig. 9 displays fiber orientation analyses of sample 1 based on the scans with the standard W target. While the color-coded illustrations of the analysis results yield a direct impression of fiber orientation, the mesh-based analysis with fiber orientation tensors per volume element produces results suitable for transfer into structural mechanics simulation software.

The color-coded illustration reveals a loss of precision that is caused by a lower voxel resolution. At the highest resolution of approximately 3 µm the course of the different fiber layers is reflected by the calculated fiber orientations. With decreasing voxel resolution the general course of fiber orientations is still described by the analysis, but a loss in detail can be observed. This is confirmed by the numerical results of fiber orientation summarized in **Tab. 4**. For the scans with the W target deviations of the fiber orientation tensors in comparison to the reference scan amount to max. 0.07. The scans of sample 1 with the Cu and the Ag target (**Fig. 10**) result in comparable deviations of the fiber orientation tensors. The relative distribution of fiber orientation components, with “xx” being the most pronounced direction, is determined correctly from all scans except the scan with the Cu target at a voxel resolution of 17 µm.

Fig. 11 and **Fig. 12** illustrate the fiber orientation analyses of samples 2 and 3. In comparison to sample 1 larger sample volumes have been scanned and the analysis regions are 6 times larger. Especially for non-homogeneous fiber-reinforced plastics, like CF-SMC, fiber orientation information over a representative sample volume is important to evaluate component quality and to have adequate input data for structural mechanics simulations. For this reason the determination of accurate fiber orientations from low-resolution CT scans is of high relevance.

Since no reference scans at high resolution exist for samples 2 and 3, only a qualitative evaluation of the results is possible. The depicted fiber orientations appear feasible for all target materials. **Tab. 5** and **Tab. 6** show minor differences of the calculated fiber orientation tensors, which are comparable in magnitude to the deviations observed for sample 1.

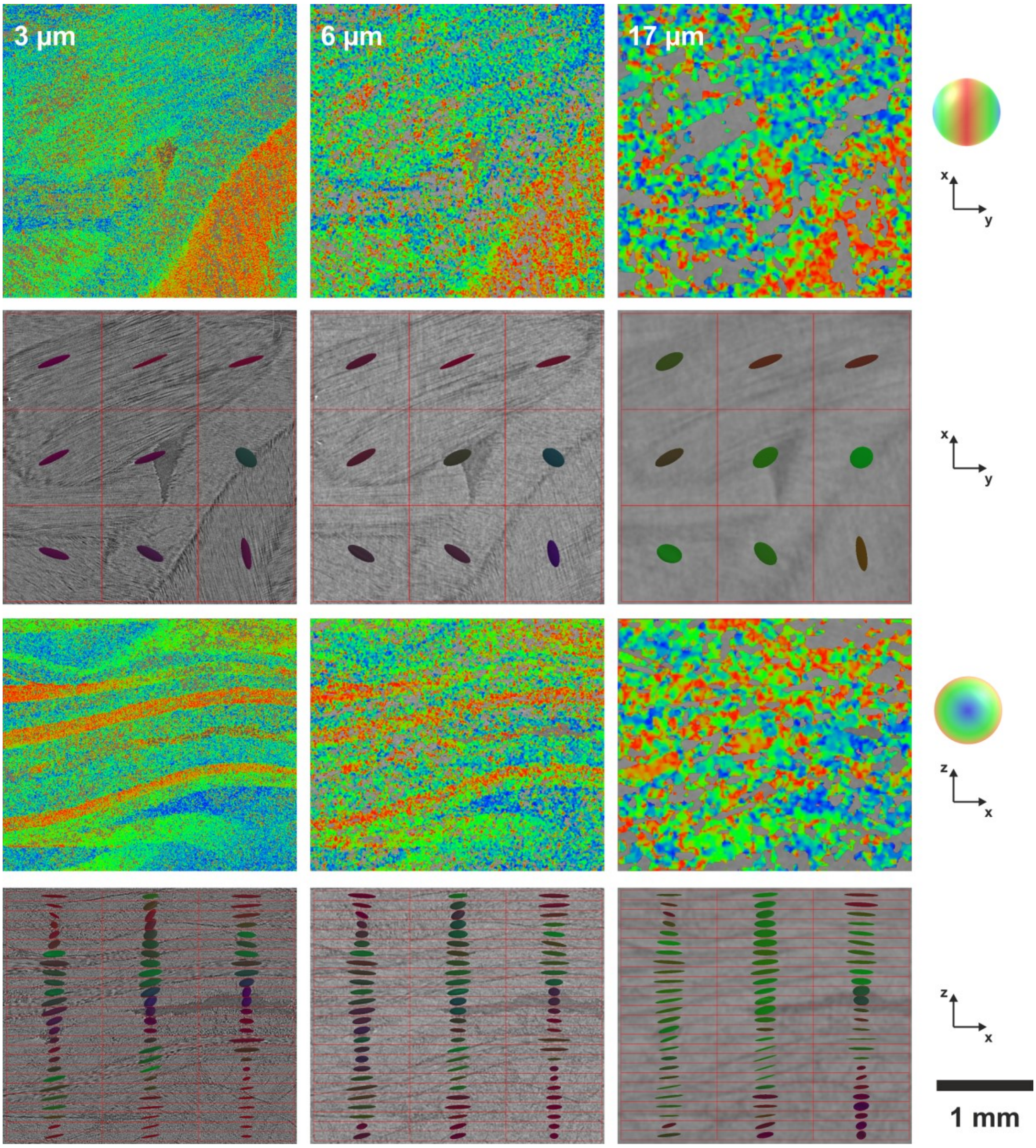

Fig. 9. Fiber orientation measurement of sample 1, W target. The color-coded images illustrate the local fiber orientations (compare globe colors for fiber orientation). The mesh-images represent the fiber orientation per unit cell. Each cell has dimensions of 1 x 1 x 0.1 mm³.

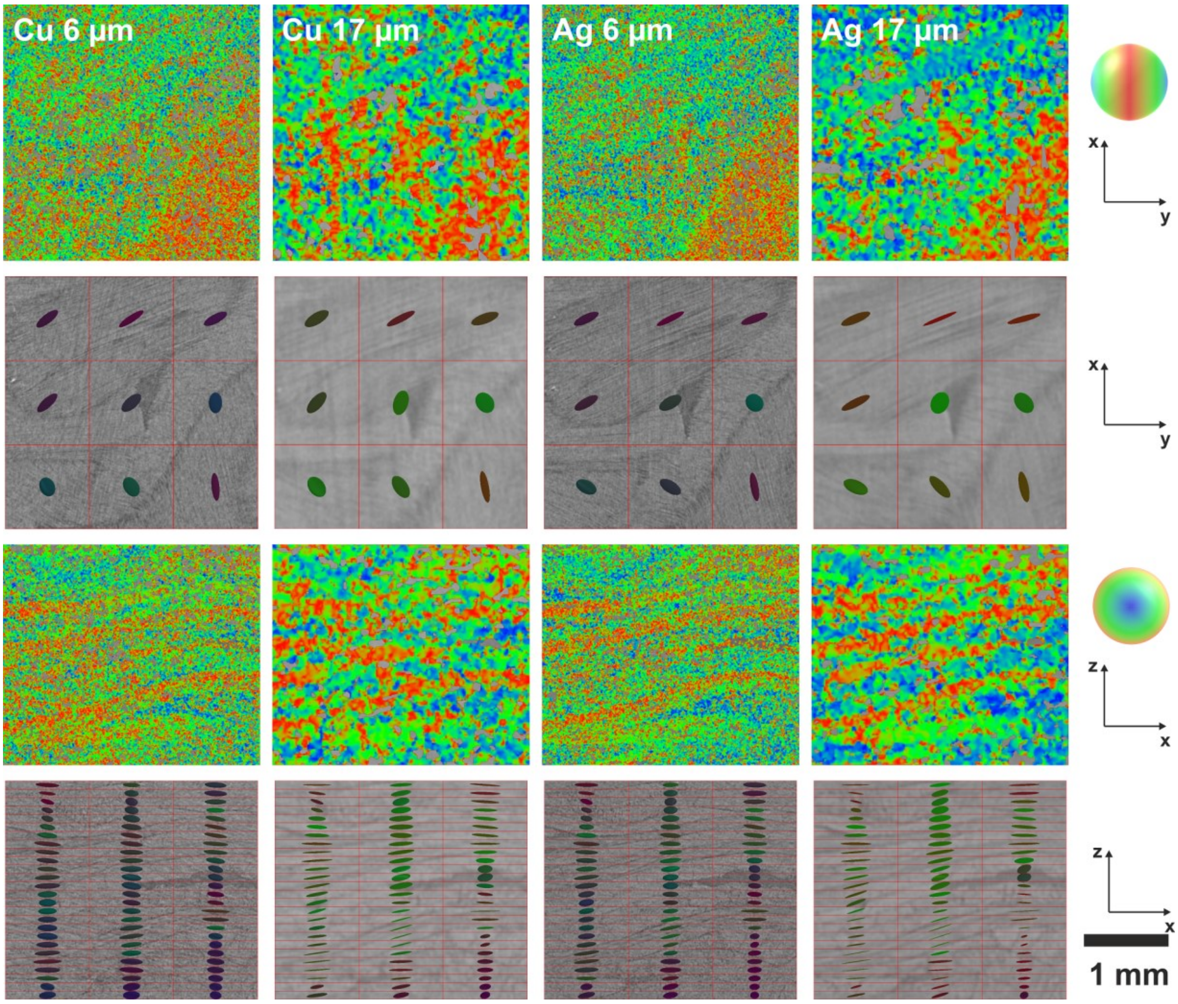

Fig. 10. Fiber orientation measurement of sample 1, Cu and Ag target. The color-coded images illustrate the local fiber orientations (compare globe colors for fiber orientation). The mesh-images represent the fiber orientation per unit cell. Each cell has dimensions of 1 x 1 x 0.1 mm³.

Tab. 4. Fiber orientation measurements of sample 1 (difference to 2.9 µm scan is given in brackets)

Target material	Voxel resolution [µm]	xx	yy	zz
W	2.9	0.36	0.54	0.10
W	6.3	0.39 (0.03)	0.52 (-0.02)	0.10 (0.00)
Cu	6.1	0.43 (0.07)	0.43 (-0.11)	0.14 (0.04)
Ag	6.1	0.39 (0.03)	0.49 (-0.05)	0.12 (0.02)
W	17.4	0.43 (0.07)	0.51 (-0.03)	0.06 (-0.04)
Cu	17.4	0.47 (0.11)	0.46 (-0.08)	0.06 (-0.04)
Ag	17.3	0.44 (0.08)	0.51 (-0.03)	0.05 (-0.05)

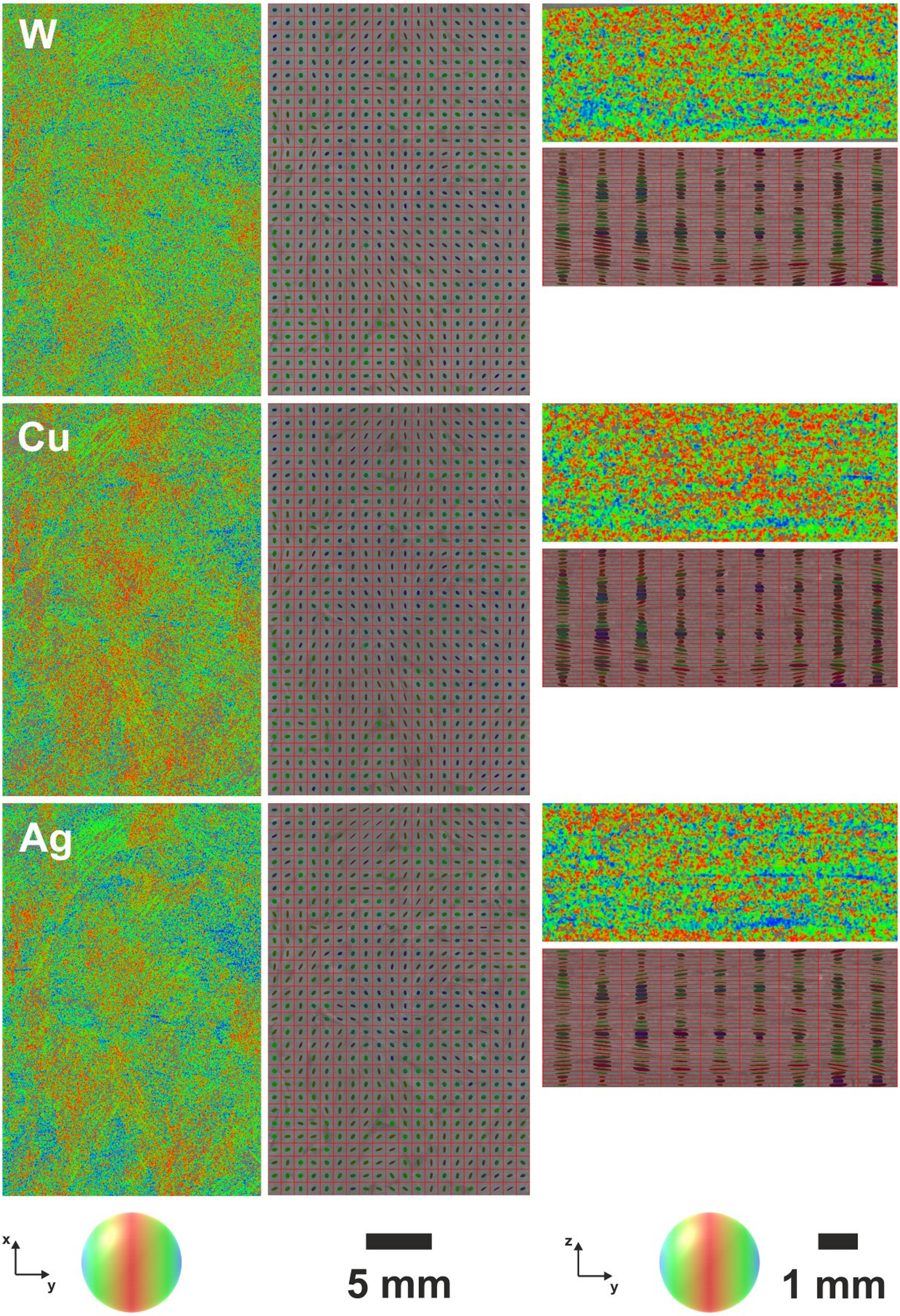

Fig. 11. Fiber orientation measurement of sample 2. The color-coded images illustrate the local fiber orientations (compare globe colors for fiber orientation). The mesh-images represent the fiber orientation per unit cell. Each cell has dimensions of 1 x 1 x 0.1 mm³.

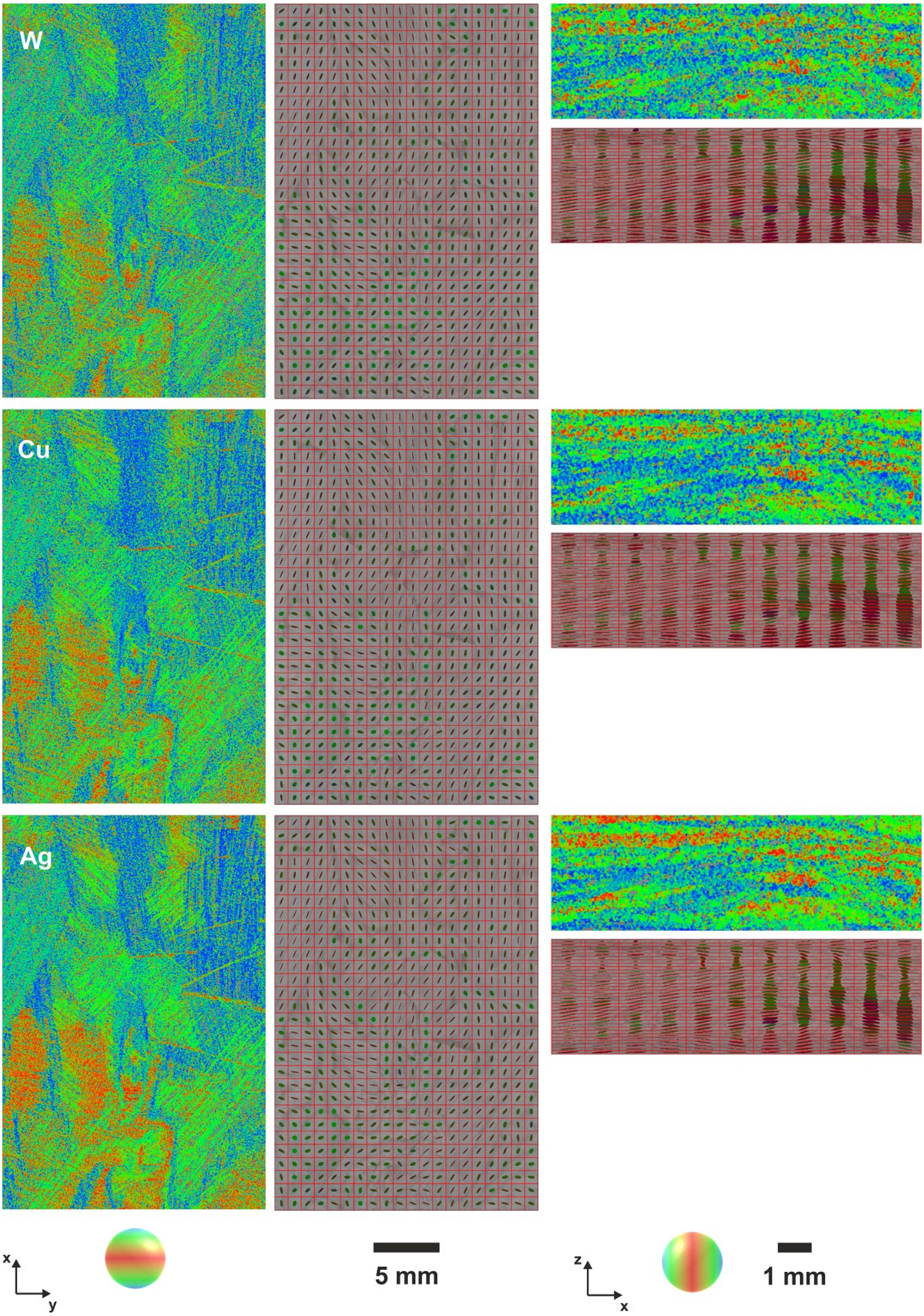

Fig. 12. Fiber orientation measurement of sample 3. The color-coded images illustrate the local fiber orientations (compare globe colors for fiber orientation). The mesh-images represent the fiber orientation per unit cell. Each cell has dimensions of 1 x 1 x 0.1 mm³.

Tab. 5. Fiber orientation measurements of sample 2

Target material	Voxel resolution [µm]	xx	yy	zz
W	17.4	0.53	0.43	0.04
Cu	17.4	0.51	0.40	0.09
Ag	17.3	0.45	0.48	0.07

Tab. 6. Fiber orientation measurements of sample 3

Target material	Voxel resolution [µm]	xx	yy	zz
W	17.4	0.54	0.40	0.06
Cu	17.4	0.53	0.41	0.06
Ag	17.4	0.49	0.47	0.04

4. Summary and Outlook

In this study three different X-ray target materials (W, Cu, and Ag) were compared regarding their performance in CT measurements of CF-SMC components.

All three target materials achieved equal resolutions using a JIMA test pattern. The CT measurements showed that Cu and Ag targets cause a shift of the grey values to slightly higher values in comparison to W target. Additional effects of the Cu and Ag target, which have to be approved, are enhanced edge contrast and, for the Ag target, improved noise levels. Because of a lower photon flux the Cu target requires about 1.5 times higher exposure times compared to the W and the Ag target to achieve comparable I_0 values.

In fiber orientation analysis no obvious advantages of the use of Cu and Ag targets could be detected. Generally the accuracy of fiber orientation analysis was observed to diminish with decreasing voxel resolution. Analyses based on scans with the Cu and Ag targets showed comparable differences to the reference high resolution scan as scans with the standard W target.

However, the general course of fiber orientations is described correctly also at a low voxel resolution of approximately 17 µm, which might be sufficient for some applications. At this voxel resolution samples with a diameter of approximately 20 mm and an even higher length have been scanned and fiber orientation analysis was performed.

Regarding the reference values for fiber orientation, a high resolution scan is assumed to deliver orientation values of high accuracy. However, no direct evidence for this assumption exists. To thoroughly evaluate the correctness of a fiber orientation analysis a reference sample of known fiber orientations would be required. Accordingly no final conclusion about the ability of the alternative target materials Cu and Ag to improve the µ-CT scan quality for fiber orientation analysis can be drawn. The development of suitable reference samples for SMC materials might be subject of further studies.

References

[1] Automobili Lamborghini S.p.A., "Technical Data Sheet Forged Composites.", 2017. Available: https://www.lamborghini.com/sites/it-en/files/DAM/lamborghini/forged/Forged%20presentation_EN.pdf. [Accessed April 23, 2019].

[2] The NORDAM Group, Inc., "Boeing 787 features composite window frames", *Reinforced Plastics,* vol. 51, no. 3, p. 4, 3 51 2007.

[3] M. Tuttle, T. Shifman and B. Boursier, "Simplifying Certification of Discontinuous Composite Material Forms for Primary Aircraft Structures", in *SAMPE*, Seattle, Washington, USA, 2010.

[4] L. De Oto, "Carbon Fiber Innovation for High Volumes - The Forged Composite", in *JEC Composites Show Paris 2011*, Paris, France, 2011.

[5] Hexcel Cooperation, "Hexcel Case Study: Audi R8 Carbon Fiber X-Brace", 2018. Available: https://www.hexcel.com/user_area/content_media/raw/HexcelCSAudiv7web(1).pdf. [Accessed April 25, 2019].

[6] B. Boursier, "New possibilities with HexMC, a high performance moulding compound", in *SAMPE Conference*, Paris, France, 2001.

[7] P. Feraboli, F. Gasco, B. Wade, S. Maier, R. Kwan, A. Masini, L. De Oto and M. Reggiani, "Lamborghini "Forged Composites®" Technology for the Suspension Arms of the Sesto Elemento", in *26th American Society for Composites (ASC) Annual Technical Conference*, Montreal, Quebec, Canada, 2011.

[8] Volkswagen AG - Group Research, Internal Documents, Wolfsburg, Germany, 2019.

[9] Hexcel Corporation, Stamford, Connecticut, USA, "HexMC User Guide", 2019. Available: https://www.hexcel.com/user_area/content_media/raw/HexMC_UserGuide.pdf. [Accessed April 23, 2019].

[10] Hexcel Corporation, Stamford, Connecticut, USA, "HexMC®-i Moulding Compound - Carbon Epoxy HexMC®-i / C / 2000 / M77." Data sheet, 2019. Available: https://www.hexcel.com/user_area/content_media/raw/HexMCi_C_2000_M77_DataSheet.pdf. [Accessed April 23, 2019].

[11] B. R. Denos and B. R. Pipes, "Local Mean Fiber Orientation via Computer Assisted Tomography Analysis for Long Discontinuous Fiber Composites", in *Proceedings of the American Society for Composites: Thirty First Technical Conference*, Williamsburg, Virginia, USA, 2016.

[12] B. R. Denos, "Fiber Orientation Measurement in Platelet-Based Composites via Computed Tomography Analysis", vol. 10608588, Purdue University, Purdue: ProQuest Dissertations Publishing, 2017.

[13] S. G. Kravchenko, "Failure Analysis in Platelet Molded Composite Systems", West Lafayette, Indiana, USA: Purdue University, School of Aeronautics and Astronautics, 2017. PhD Thesis.

[14] S. C. Garcea, Y. Wang and P. J. Withers, "X-ray computed tomography of polymer composites", *Composites Science and Technology,* vol. 156, pp. 305-319, 2018.

[15] H. Shen, S. Nutt and D. Hull, "Direct observation and measurement of fiber architecture in short fiber-polymer composite foam through micro-CT imaging", *Composites Science and Technology,* vol. 64, no. 13, pp. 2113-2120, 2004.

[16] T. Riedel, "Evaluation of 3D fiber orientation analysis based on x-ray computed tomography data", in *Conference on Industrial Computed Tomography (ICT)*, Wels, Austria, 2012.

[17] S. Goris and T. A. Osswald, "Progress on the characterization of the process-induced fiber microstructure of long glass fiber-reinforced thermoplastics", in *Proc 16th SPE Automot Compos Conf Exhib (ACCE)*, Novi, Michigan, USA, 2016.

[18] D. Maier, T. Dierig, C. Reinhart and T. Günther, "Analysis of Woven Fabrics and Fiber Composite Material Aerospace Parts using Industrial CT Data", in *5th International Symposium on NDT in Aerospace*, Singapore, 2013.

[19] L. Brömstrup, "Fließpresssimulation kohlenstofffaserverstärkter Sheet Molding Compounds – Potentialanalyse der Einzelfasersimulation", Bachelor Thesis, Volkswagen AG, Wolfsburg, 2018.

[20] B. R. Denos, D. E. Sommer, A. J. Favaloro, B. R. Pipes and W. B. Avery, "Fiber orientation measurement from mesoscale CT scans of prepreg platelet molded composites", *Composites Part A: Applied Science and Manufacturing,* vol. 114, pp. 241-249, 2018.

[21] A. Schulman. Technical Data Sheet, "https://engineeredcomposites.aschulman.com/data-sheets", 2019. Available: https://cdn2.hubspot.net/hubfs/2015678/Engineered%20Composites%20/Documents/Product%20PDFs/Quantum/ASI-TDS-AMC%208593%20HT%20rev.pdf. [Accessed May 6, 2019].

[22] JIMA, "Japan Inspection Instruments Manufacturers' Association", Available: http://www.jima.jp/english/assen-e.html. [Accessed May 2, 2019].

[23] N. Flay and R. Leach, "Application of the optical transfer function in X-ray computed tomography – a review", National Physical Laboratory (NPL), Report ENG 41, Teddington, Middlesex, United Kingdom, 2012.

[24] C. Bellon and G.-R. Jaenisch, "aRTist – Analytical RT Inspection Simulation Tool", in *DIR 2007 - International Symposium on Digital industrial Radiology and Computed Tomography*, Lyon, France, June 25-27, 2007.